Oncology
and Radiotherapy ©

18(3) 2024: 001-012 • RESEARCH ARTICLE

A comparison study of profile measurements of unflatten photon beams utilizing various detector arrays

Mr. Kanakavel Kandasamy[1], **E. James Jebaseelan Samuel**[2]

[1] Research Scholar, Department of Physics, School of Advanced Sciences, VIT Vellore, India
[2] Higher Academic Grade, Department of Physics, and School of Advanced Sciences, VIT Vellore, India

ABSTRACT

Introduction: For routine beam profile analysis of a linear accelerator, two-dimensional array detectors are used to characterize the beam's flatness, symmetry, radiation field size, and penumbra of a given photon-flattening filter beam. However, the objective of this research was to assess the suitability of various array detectors by comparing the dosimetric parameters of an FFF beam profile.

Materials and Methods: Profiles were measured utilizing the 729, 1500, 1600, Starcheck arrays, Pinpoint 3D with Beamscan system, and EPID Panel. A 100 MU radiation dose was applied to 6FFF and 10FFF beams with square fields of 10 cm^2 x 10 cm^2, 15 cm^2 x 15 cm^2, and 20 cm^2 x 20 cm^2, respectively, using a Varian True Beam Linear Accelerator. All detectors kept at the isocenter of the Linac to be unique. Dosimetric parameters, including FWHM, off-axis ratio, degree of unflatness, penumbra, and symmetry, were extracted from measured FFF beam profiles utilizing PTW Beamscan software.

Results: In terms of field size, the 729 array exhibited the greatest deviation from nominal field size at 10 cm^2 x 10 cm^2 for both FFF beams in FWHMs. 1.05 mm represented the greatest possible deviation for the 729 array. In comparison to the even field diameters of 10x10 cm^2 and 20 cm^2 x 20 cm^2, the 729 array exhibited the greatest FWHM deviation. With the 1500 array, however, the effect was the exact opposite. A maximum difference of 1.49 mm was recorded in the 15 cm^2 x 15 cm^2 field, while the remaining two fields exhibited differences of less than 1 mm. It was determined that the maximal degree of unflatness for the 1600SRS and 729 arrays was 10.8 mm and 9.72 mm, respectively, in comparison to the Pinpoint 3D chamber. A declining trend was identified in the Penumbra analysis, commencing with the 729, followed by the 1500, 1600SRS, Starcheck, Pinpoint 3D, and EPID detectors. An elevation of approximately 13 mm was recorded for the 729 array, while the EPID recorded 3 mm. Conversely, it was demonstrated that the beam symmetry and OAR of every detector array were below 1%.

Conclusion: It is evident from the research that the resolution of the array detector is the most crucial factor when conducting profile measurements using the FFF beam and the depth of detectors placed in each array also played a big role. With the exception of (729, 1500, and 1600) arrays, Starcheck and EPID outcomes were remarkably comparable to those of IEC 60976 and Pinpoint 3D.

Keywords: degree of unflatness, planar detector arrays, inflection point, flattening filter free beam, AERB task group

Address for correspondence:
E. James Jebaseelan Samuel, Higher Academic Grade, Department of Physics, School of Advanced Sciences, VIT Vellore, India
E-mail: ejames@vit.ac.in

Word count: 5335 **Tables:** 10 **Figures:** 12 **References:** 42

Received: 08 March, 2024, Manuscript No. OAR-24-129135
Editor assigned: 10 March, 2024, Pre-QC No. OAR-24-129135 (PQ)
Reviewed: 20 March, 2024, QC No. OAR-24-129135 (Q)
Revised: 25 March, 2024, Manuscript No. OAR-24-129135 (R)
Published: 31 March, 2024, Invoice No. J-129135

INTRODUCTION

Modern linear accelerators having Flattening Filter Free (FFF) beams are majorly nowadays being used for treatment techniques especially for Stereotactic Body Radiation therapy (SBRT), Stereotactic Radiosurgery (SRS), and Volumetric Modulated Arc therapy (VMAT). By eliminating the flattening filter from the path of radiation emanating from the radiation source, the dose rate is multiplied by a factor of two to four. The outcomes consist of decreased mean energy and treatment time, as well as decreased head leakage and lateral dispersal, all of which have demonstrated their benefits in specialized treatment procedures. The absence of beam hardening effects results from the transformation of a beam into an FFF beam upon removal of the flattening filter. These results are as follows: (1) an increase in dose- or pulse-induced photon energy fluence for FFF beams; and (2) off-axis spectra that are not significantly different from those of the central axis for the FFF beam, as opposed to a substantial shift in spectrum caused by the flattening filter [1-4]. When selecting a detector to measure absolute and relative doses in the presence of high-dose rate beams, certain obstacles have always existed [5]. In a similar fashion, the spatial distance concept utilized for conventional beams to determine the penumbral widths of unflattened beams between 80% and 20% dose values is no longer applicable to profile measurement [6]. Diverse studies have documented that inflection point analysis for an unflattening beam profile is the most effective method for deriving and analyzing FFF beam parameters in order to circumvent this issue [7-10]. An analysis method for evaluating the FFF beam profile was also developed by G. Sahani, S. D. Sharma, and others. This method considered various parameters, including the radiation field size, degree of unflatness, penumbra, symmetry, and off-axis ratio. This was subsequently recommended by the Atomic Energy Regulatory Board Task Group (AERB) [11]. The results of this investigation were obtained through the utilization of a Radiation Field Analyzer (RFA) equipped with a single ionization chamber featuring a sensitive volume of approximately 0.13 cc. In an abundance of additional investigations, only RFA and an ionization chamber were utilized. Conversely, several investigations employed diverse two-dimensional array detectors to conduct profile measurements for Flattening Filter (FF) photon beams [12-16]. However, the literature does not provide any substantiation

regarding the use of these arrays for FFF beam profiles. This research focuses on the utilization of various 2D detector arrays to measure FFF beam profiles and compares the dosimetric results of these profiles to those of RFA measurements with single detector utilizing AERB Task group

MATERIALS

Linear accelerator

Measurements were taken using a TrueBeam™ system, a high-end modal linear accelerator from Varian Medical System, with both flattened and unflattened beams [17]. The Linac produceS photon energies of X6, X6FFF, X10, X15, and X10FFF. The field sizes range from 1 cm^2 × 1 cm^2 to 40 cm^2 × 40 cm^2 embedded in the Linac. The maximal dose rates used in the Linac are 600, 1600, and 2400 MU/min for FF, X6FFF, and X10FFF beam energies, respectively.

Measuring tools

In this study, we used Octavius Detector arrays (729, 1500, and 1600 SRS), as well as PTW Dosimetry Company's Starcheck [18-21]. In addition to the arrays listed above, Varian's amorphous silicon Digital Megavolt Imager (DMI), also known as the Electronic Portal Imaging Device (EPID) with Portal Dosimetry, was used [22]. Table 1 lists all measurement devices and their associated parameters. Figure 1 illustrates the resolution differences among array systems. A Real Water (RW3) slab phantom (white dense polystyrene material ρ =1.045 g/cm^3) with a thickness of 1 cm, a 2 cm chamber, and 1 mm and 2 mm plates were utilized to establish detector arrays at their reference point of measurement (as per manufacturer specifications) [23]. To measure and extract beam profiles, PTW Verisoft software, Beamscan software with scan data, and the image analysis module were utilized in the relevant locations [24-25]. A Pinpoint 3D chamber (T31022) was used for profile measurement along the PTW Beamscan 3D RFA System, which served as the reference measurement for intercomparison [21].

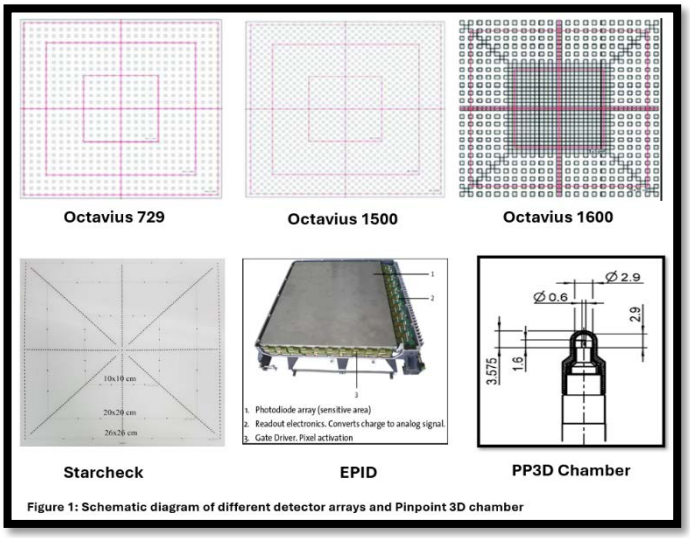

Fig. 1. Measuring tools

METHODS

Measurement setup

For this investigation, only X6FFF and X10FFF energies were used. Prior to measurement, the Linac's output and beam profiles were set in accordance with the international standard IEC 60976 [26, 27]. All PTW 2D arrays and their Effective Point of Depth (as shown in Table 1) were maintained on RW3 slabs at 5 cm depth, with 1 mm and 2 mm plates used for accurate setup. To provide proper scatter from the array's rear side, 10 cm slabs were put. Common beam parameters such as 10 cm^2 × 10 cm^2, 15 cm^2 × 15 cm^2, and 20 × 20 cm^2 were used, as well as a Source to Axis Distance (SAD) of 100 cm. All arrays were irradiated with 100 MU. Similarly, the DMI panel was transported to the Linac Isocenter Point (SAD) and delivered with the same 100 MU. The exposed image file for the corresponding irradiation was exported as DICOM files. These DICOM files were evaluated using Beamscan's Film and Image Analysis program, and profiles were developed. Except for the other detectors, because the 1600 SRS array has a field size constraint of 15 cm^2 × 15 cm^2, the array was configured so that the diagonal axis of the array corresponded to the primary axis of 20 cm^2 × 20 cm^2, and the measurement was taken. The maximum field size for a 1600 array is 20 cm^2 × 20 cm^2, hence it was used as the largest field for all arrays. In contrast, the Pinpoint 3D chamber was fixed at a depth of 5 cm with a 95 cm SSD in the Beamscan system. Profiles were scanned for all indicated file sizes, and data was extracted. To make the study simple, only Inline profiles were considered for evaluation. As a precondition, all arrays and the Pinpoint 3D Chamber were given a 2Gy pre-irradiation dose and zeroed for high reproducibility. For the DMI Panel, image and dosimetric calibration were carried out in accordance with the vendor's guidelines [28].

Tab. 1. Technical details of different detector arrays

Detector Modal	Detector type	Technical details
Octavius 729	Vented Ion Chamber	Chamber Volume and Nos: 0.125 cc & 729
		Field Size Coverage : 2 cm^2 × 2 cm^2 to 27 cm^2 × 27 cm^2
		Resolution of the array : 10 mm
		Dose Rate range : 3 Gy/min to 48 Gy/min
		Energy Range : (Co ... 25) MV
		Effective Point of Depth : 7.5 mm from Surface
Octavius 1500	Vented Ion Chamber	Chamber Volume and Nos : 0.125 cc & 1405
		Field Size Coverage : 2 cm^2 × 2 cm^2 to 27 cm^2 × 27 cm^2
		Resolution of the array : 7.07 mm(Diagonal Axis)
		Dose Rate range : 3 Gy/min to 48 Gy/min
		Energy Range : (Co ... 25) MV
		Effective Point of Depth : 7.5 mm from Surface
[a]Octavius 1600 SRS	Liquid Filled Ion Chamber	Chamber Volume and Nos : 0.125 cc & 1521
		Field Size Coverage : 1 cm^2 × 1 cm^2 to 15 cm^2 × X15 cm^2
		Resolution of the array : 5 mm (>6.5X6.5 cm^2)
		Dose Rate range : 0.8 Gy/min to 24 Gy/min
		Energy Range : (Co ... 25) MV
		Effective Point of Depth : 9 mm from Surface
Starcheck	Vented Ion Chamber	Chamber Volume and Nos : 0.125 cc & 527
		Field Size Coverage : 4 cm^2 × X4 cm^2 to 26 cm^2 × X26 cm^2
		Resolution of the array : 3 mm
		Dose Rate range : 2 Gy/min to 80 Gy/min
		Energy Range : (Co... 25) MV
		Effective Point of Depth : 8.5 mm from Surface
Pinpoint 3D (T31022)	Vented Ion Chamber	Volume : 0.016 cc
		Energy Range : Co ... 25 MV photons
		Measurement Resolution : 1 mm
		Field size : 2 cm^2 × 2 cm^2 to 40 cm^2 × × 40 cm^2
		Max Dose Rate : 91.6 Gy/s
Varian DMI	Amorphous Silicon detector	Field Size Coverage : up to 43 cm^2 × 43 cm^2
		Resolution of EPID DMI : 0.3 mm
		Energy Range : (Co... 25) MV
		Effective Point of Depth : 8.5 mm from Surface

The measuring length at the diagonal axis of the 1600 SRS array is a 21 cm.

Measurement parameters

Full Width Half Maximum (FWHM):

From measured data samples of all devices, PTW Beamscan software is used to calculate FWHM through the inflection point. In the software, new data points are added to the existing measuring points by linear interpolation so that equidistant data points are obtained. In the next step, the curve is smoothed. The smoothing operation blurs the penumbra, but its effect on the X-values of the inflection points (position) is negligible. The first derivative of the smoothed curve is calculated. A brute-force search is employed to search for the global maximum of the first derivative. In order to eliminate the effect of noise, all neighbouring points of this maximum are considered whose derivative exceeds a threshold (e.g., half the maximum) and that provide a weighted average of their X-

values. The X-values (positions) of the left and right inflection points are determined. The corresponding Y-values are calculated from the original curve by linear interpolation, with the Y-values of the left and right inflection points not necessarily being the same. Then, the two Y values are averaged. The X-values (positions) are corrected (by linear interpolation) so that they correspond to the averaged Y-value. Finally, FWHMs are deduced [29].

Symmetry:

The field symmetry of a beam is defined as the largest absolute change in radiation intensity between any two symmetric sites around the beam midline inside the centre 80% of the field, given as a percentage of the mean radiation intensity, according to IEC 60976 [27].

$$Symmetry = \left(\frac{D(x)}{D(-x)}\right) \max * 100\ \%$$

Penumbra:

The area around the edge of a radiation beam where the dose changes rapidly in relation to the distance from the beam axis is called the penumbra. The physical penumbra width is the distance between the 20% and 80% isodose curves at a specific depth, comprising the geometrical, transmission, and radiological penumbra components. The AERB Task Group states that for FFF Beams, the penumbra should be determined using the dosage value at the Inflection Point (IP) as the Reference Dose Value (RDV). Points Pa and Pb, located at 1.6 and 0.4 times the RDV, respectively, need to be found according to Figure 2. The penumbra will be measured by the lateral spacing between Pa and Pb on each side of the profile [11].

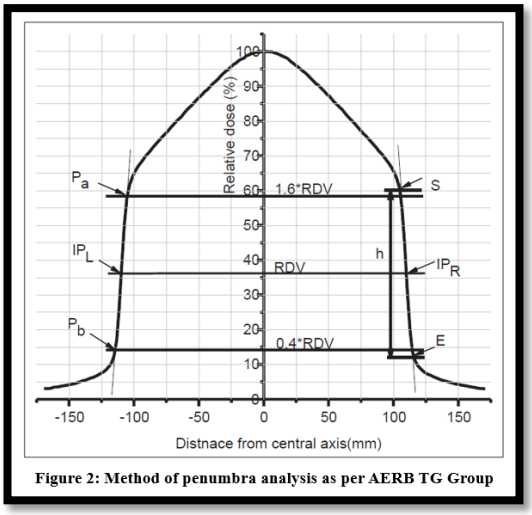

Fig. 2. Method of penumbra analysis as per AERBTG group

Degree of unflatness:

According to AERB Task Group to quantify the degree of unflatness, the lateral distance from the central axis at 90%, 75% and 60% dose points on either side of the beam profile shall be recorded along major axes for all available beam energies (Figure 3) [11].

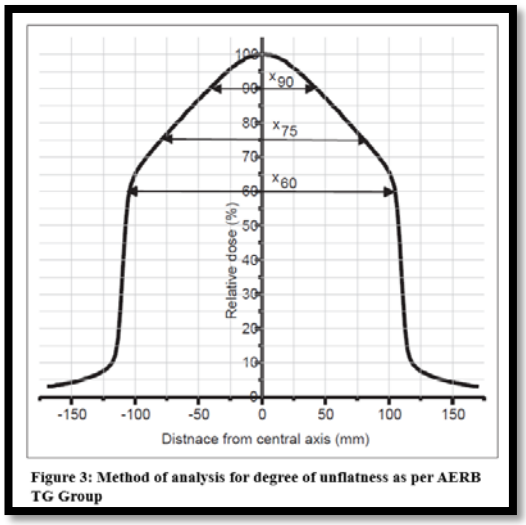

Fig. 3. Method of analysis for degree of unflatness as per AERBTG group

Off-axis ratio:

As per AERB Task Group OAR at ± 3 cm from central axis for 10 cm × 10 cm collimator setting shall be measured and tabulated for all available un-flat beam energies [11].

RESULTS AND DISCUSSION

Profiles were taken from each detector's measurement and graphically presented, as seen in the (Figure 4a, 4b, 5a, 5b, 6a, & 6b) for both photon 6FFF and 10FFF beams. Data from beamscan software analysis utilizing these profiles was collected and tabulated in (Table 2-10) for FWHM, symmetry, penumbra, degree of unflatness, and off-axis ratio for both 6FFF and 10FFF photon beams respectively.

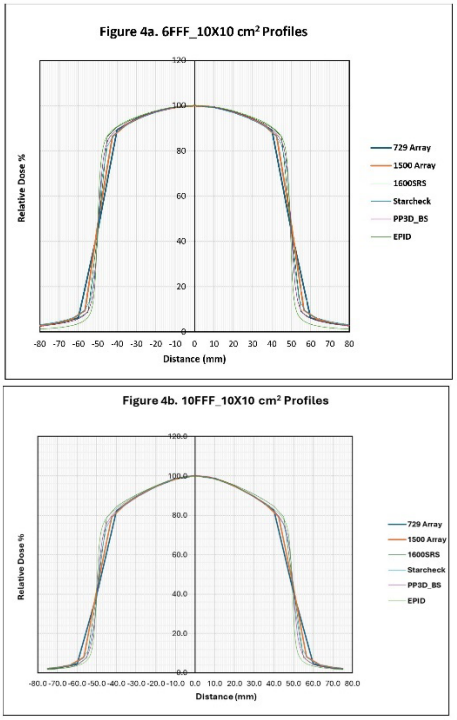

Fig. 4 a) 6FFF_10 cm^2 × 10 cm^2 profiles b. 10FFF_10 cm^2 × 10 cm^2 profiles

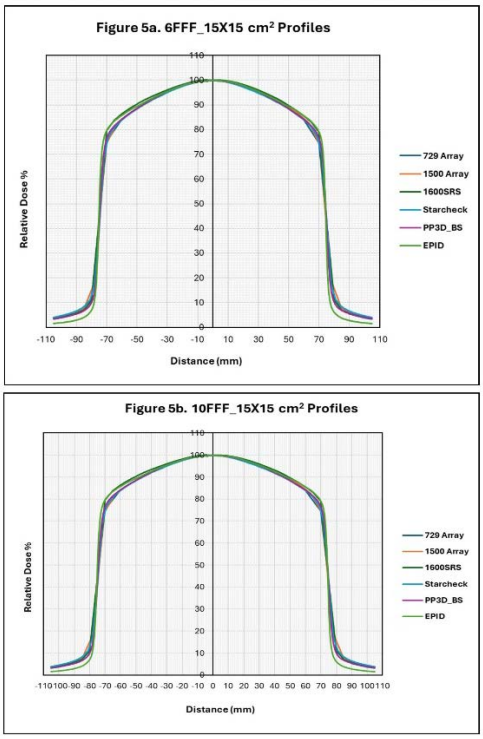

Fig. 5 a) 6FFF_15 cm^2 × 15 cm^2 profiles b. 10FFF_15 cm^2 × 15 cm^2 profiles

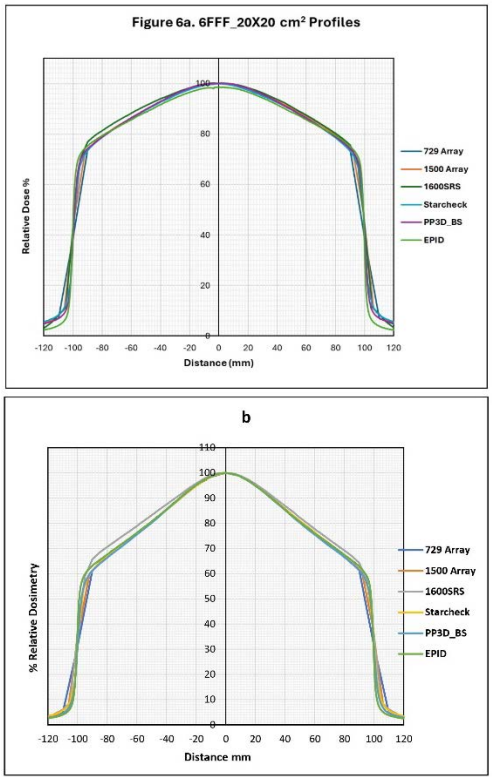

Fig. 6 a) 6FFF_20 cm² × 20 cm² profiles, b. 10FFF_20 cm² × 20 cm² profiles

Tab. 2. Measured FWHM in cm for 6FFF beam

	FWHM vs Detectors		
	10	15	20
729 Array	9.92	14.99	19.94
1500 Array	9.95	14.86	19.97
1600 SRS	9.96	14.98	20.05
Starcheck	9.97	14.97	19.95
PP3D	9.97	14.98	19.99
EPID	9.95	14.98	20

Tab. 3. Measured FWHM in cm for 6FFF beam

	FWHM vs Detectors		
	10	15	20
729 Array	9.9	14.99	19.92
1500 Array	9.93	14.85	19.94
1600 SRS	9.95	14.98	20.03
Starcheck	9.97	14.96	19.93
PP3D	9.96	14.97	19.97
EPID	9.94	14.98	19.99

Tab. 4. 6FFF Measured Penumbra (Averaged for Left & Right)

	Detector Arrays vs Average Penumbra (in mm)		
	10	15	20
729 Array	13.52	8.11	14.31
1500 Array	10.82	7.56	12.08
1600 SRS	7.21	7.84	8.72
Starcheck	6.34	6.19	8.66
PP3D	4.93	5.23	5.51
EPID	3.22	3.37	3.48

Tab. 5. 10FFF Measured Penumbra (Averaged for Left & Right)

	Detector Arrays vs Average Penumbra (in mm)		
	10	15	20
729 Array	13.15	8.13	13.79
1500 Array	10.64	7.45	11.65
1600 SRS	7.26	7.77	8.53
Starcheck	6.31	6.13	8.32
PP3D	5.2	5.38	5.71
EPID	3.22	3.31	3.53

Tab. 6. Measured Degree of unflattens and its difference among different detectors for 6FFF Beam

	Degree of unflatness_6FFF in cm								
	10 cm² × 10 cm²			**15 cm² × 15 cm²**			**20 cm² × 20 cm²**		
	X-90%	X-75%	X-60%	X-90%	X-75%	X-60%	X-90%	X-75%	X-60%
729 Array	7.72	8.65	9.32	9.21	13.96	14.47	9.75	17.54	18.79
1500 Array	7.52	8.94	9.53	9.36	13.93	14.5	9.96	17.69	19.13
1600SRS	8.11	9.27	9.63	9.97	14.12	14.54	10.56	18.18	19.37
Starcheck	7.54	9.33	9.74	9.15	13.59	14.6	9.74	17.48	19.42
PP3D	7.8	9.48	9.78	9.26	14.14	14.7	9.27	17.63	19.56
EPID	8.21	9.62	9.83	9.6	14.43	14.8	9.91	18.44	19.74
	Difference in Degree of unflatness_6FFF with respect to PP3D in mm								
	10 cm² × 10 cm²			**15 cm² × 15 cm²**			**20 cm² × 20 cm²**		
	X-90%	X-75%	X-60%	X-90%	X-75%	X-60%	X-90%	X-75%	X-60%
729 Array	0.84	8.35	4.62	0.51	1.79	2.3	4.79	0.86	7.71
1500 Array	2.77	5.43	2.54	1.04	2.1	2.03	6.84	0.6	4.31
1600SRS	3.08	2.06	1.48	7.1	0.23	1.56	12.84	5.5	1.91
Starcheck	2.66	1.5	0.39	1.05	5.52	0.95	4.65	1.46	1.42
EPID	4.09	1.37	0.51	3.39	2.85	1.02	6.31	8.15	1.76

Tab. 7. Measured Degree of unflattens and its difference among different detectors for 10FFF Beam

10FFF_Degree of unflatness in cm									
	10 cm^2 × **10** cm^2			**15** cm^2 × **15** cm^2			**20** cm^2 × **20** cm^2		
	X-90%	X-75%	X-60%	X-90%	X-75%	X-60%	X-90%	X-75%	X-60%
729 Array	5.755	8.352	9.065	6.06	11.726	14.139	6.149	12.343	18.091
1500 Array	5.729	8.657	9.283	6.078	11.767	14.226	6.171	12.498	18.386
1600SRS	6.157	9.106	9.502	6.61	12.663	14.289	6.709	13.586	18.763
Starcheck	5.678	8.497	9.621	5.985	11.776	14.299	6.077	12.455	18.303
PP3D	5.779	9.033	9.655	6.039	11.667	14.358	6.115	12.218	18.34
EPID	5.883	9.331	9.758	6.14	12.021	14.625	6.199	12.506	18.884
Difference in Degree of unflatness with respect to PP3D in mm									
	10 cm^2 × 10 cm^2			**15 cm^2 × 15 cm^2**			**20 cm^2 × 20 cm^2**		
	X-90%	X-75%	X-60%	X-90%	X-75%	X-60%	X-90%	X-75%	X-60%
729 Array	0.24	6.81	5.9	0.21	0.59	2.19	0.34	1.25	2.49
1500 Array	0.5	3.76	3.72	0.39	1	1.32	0.56	2.8	0.46
1600SRS	3.78	0.73	1.53	5.71	9.96	0.69	5.94	13.68	4.23
Starcheck	1.01	5.36	0.34	0.54	1.09	0.59	0.38	2.37	0.37
EPID	1.04	2.98	1.03	1.01	3.54	2.67	0.84	1.25	5.44

Tab. 8. Measured Symmetry (%) for 6FFF Beam

	10 cm^2 × 10 cm^2	**15 cm^2 × 15 cm^2**	**20 cm^2 × 20 cm^2**
729 Array	100.14	100.19	100.33
1500 Array	100.2	100.55	100.52
1600SRS	100.47	100.86	101.36
Starcheck	100.45	100.45	100.43
PP3D	100.3	100.35	100.34
EPID	100.26	100.46	100.52

Tab. 9. Measured Symmetry (%) for 10FFF Beam

	10 cm^2 × 10 cm^2	**15 cm^2 × 15 cm^2**	**20 cm^2 × 20 cm^2**
729 Array	100.3	100.3	100.3
1500 Array	100.2	100.5	100.3
1600SRS	100.2	101.3	102
Starcheck	100.2	100.4	100.4
PP3D	100.4	100.4	100.4
EPID	100.3	100.3	100.5

Tab. 10. Measured OAR (%) for both 6FFF and 10FFF Beam

	6FFF	**10FFF**
729 Array	94.14	89.35
1500 Array	93.99	89.15
1600 SRS	94.66	90.44
Starcheck	93.66	89.04
PP3D	94.18	89.34
EPID	94.94	89.77
Average	94.26	89.51
Standard Deviation	0.47	0.52

In terms of field size, Figure 7 and 8 shows the overall difference in FWHMs between all detectors for both 6FFF and 10FFF Beams. When compared to the nominal field size, the 729 array with 10 mm resolution showed the greatest difference at 10 cm^2 × 10 cm^2 for both FFF beams in FWHMs. The maximum difference for the 729 array was 1.05 mm. For even field sizes of 10 cm^2 × 10 cm^2 and 20 cm^2 × 20 cm^2, the 729 array was found to have a larger FWHM deviation. There are two reasons why this impact occurs. One is the detector resolution of the array, which is lacking the actual radiation field edge. The other issue is that the field border of the provided field did not automatically align with the chamber position due to the effective depth of arrays where detectors are situated. In contrast, for 15 cm^2 × 15 cm^2, no effect was detected. Because the chamber was located at the radiation field edge, So, the 729-array exhibited <1mm deviation. However, for a 1500-array with a resolution of 7 mm, the impact was opposite. The largest variation of 1.49 mm was reported for 15 cm^2 × 15 cm^2 and less than 1 mm for the other two fields. Other detectors, including the 1600 SRS array, Starcheck, Pinpoint 3D, and EPID, showed deviations of less than 0.5 mm. Our observations and analysis revealed that using a detector with a better measurement resolution resulted in more accurate FWHM measurements. Furthermore, with the exception of the Starcheck and EPID detector arrays, the effective build-up depths of the other arrays (729, 1500, and 1600) differed. According to Pichandi et al., the 50% intensity level is recorded in the steeply dropping portion of the beam profile, which is a high-gradient area [6]. The field dimension of FFF beams differs from the standard notion. As Falk Ponisch et al. and Fogliata et al. have previously explained, the resolution of measurements was the sole reason for this disparity [10, 30]. The higher the resolution, the lower the fluctuation in FWHMs.

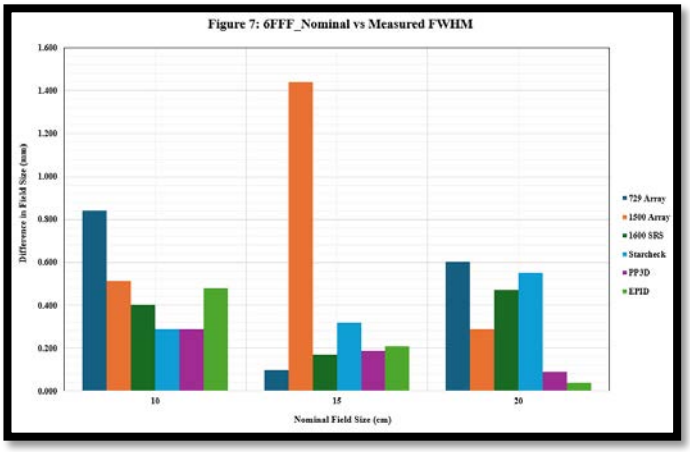

Fig. 7. 6FFF_Nominal vs measured FWHM

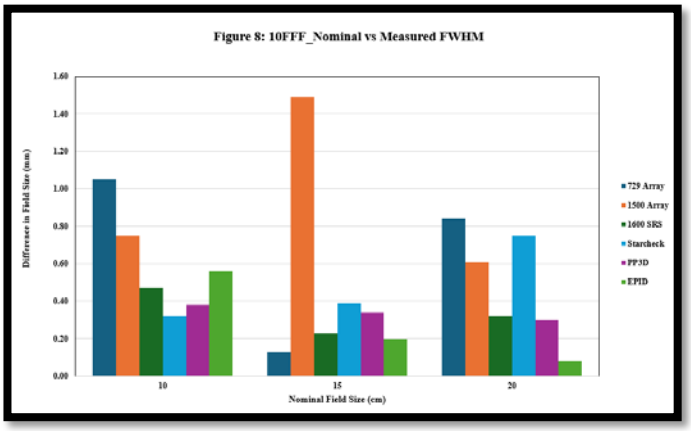

Fig. 8. 10FFF_Nominal vs measured FWHM

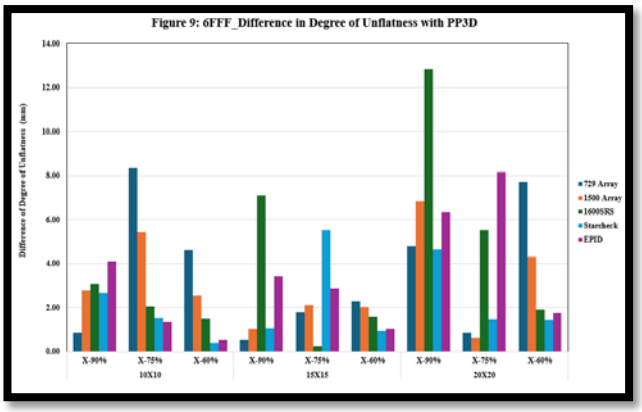

Fig. 9. 6FFF_Difference in degree of unflatmess with PP3D

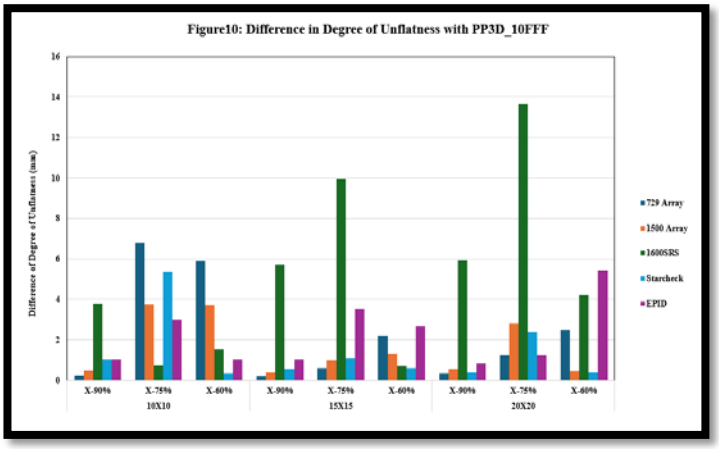

Fig. 10. Difference in degree of unflatmess with PP3D_10FFF

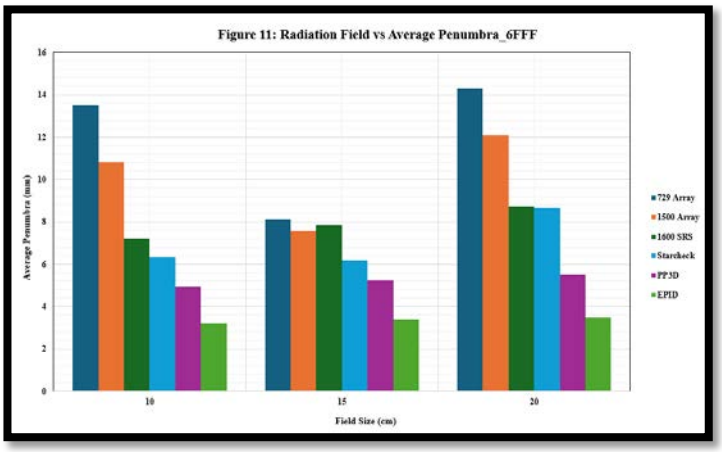

Fig. 11. Radiation field *vs* average penumbra_6FFF

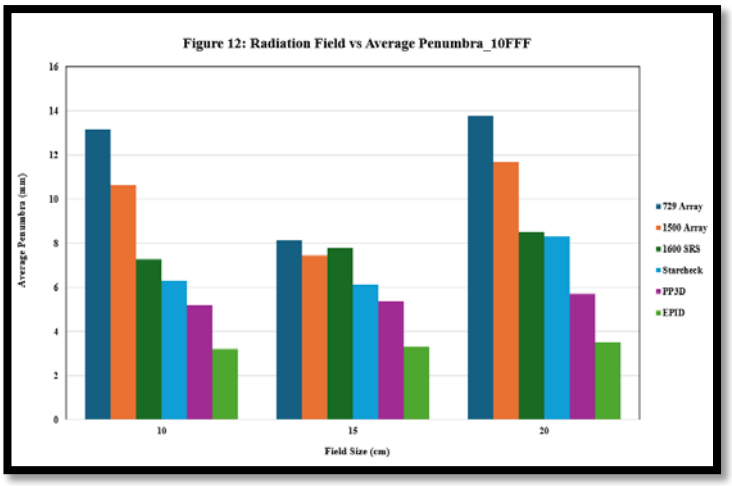

Fig. 12. Radiation field *vs* average penumbra_10FFF

Whereas there is no standard data for degree of unflatness, the pinpoint 3D measurements in the Beamscan water phantom were used as a reference for comparison. When compared to the Pinpoint 3D chamber, the degree of unflatness was found to be the highest at 10.8 mm for the 1600SRS and 9.72 mm for the 729 arrays. This was clearly noticed in the following (Figure 9 and 10) to determine differences between detector arrays. This discrepancy also demonstrated that array resolution is the cause of the deviation.

In the Penumbra study, a declining trend was seen beginning with the 729, 1500, 1600SRS, Starcheck, Pinpoint 3D, and EPID detectors. The 729 arrays had the highest penumbra, measuring around 13 mm, while the EPID had a penumbra of about 3 mm. This was attributable only to detector resolution. The penumbra was noted to be less as resolution increased. The generic penumbra must be less than 10 mm, according to IEC 60976 [27]. Except for the 729 and 1500 arrays, all other detectors are equivalent to one another and within the limit. The Figures 11, 12 explain about the penumbral variation among detector arrays for both the Beams.

In contrast, for both 6FFF and 10FFF energies, the beam symmetry of all detector arrays was less than 1%, with the exception of the 1600 SRS array (>1%) refer the (Table 8 and 9). According to IEC 60976, the symmetry of a photon beam for a given field size must be less than 103%, and overall symmetry must be within acceptable limits [27]. As shown in the Table 10, the highest standard deviation in Off Axis Ratio (OAR) for 10 cm^2 × 10 cm^2 was less than 0.5 across all detectors for both photon FFF energies [11].

CONCLUSIONS

The detector arrays in this investigation yielded varying findings in terms of FWHM, penumbra, and degree of unflatness, while showing little differences in symmetry and off-axis ratio. The resolution of the array detectors significantly influenced the FWHM, penumbra, and degree of unflatness. Therefore, it is clear that the resolution of the array detector is crucial for profile measurements in FFF Beam. Starcheck and EPID results were comparable to IEC 60976 and Pinpoint 3D standards, except for the 729, 1500, and 1600 SRS array models. One can utilize 729, 1500, and 1600 SRS arrays for consistency measurement to conduct trend analysis, following the guidelines in the AAPM TG 142 standard, by carefully selecting the radiation field size, as outlined in this paper. One should analyse the dosimetric benefits of a planar array for regular quality assurance tests prior to its use. PTW Starcheck and EPID with dosimetry options, which are compatible with high dose rates, are suitable alternative instruments for regular profile measurement and analysis as compared to a radiation field analyser with single detector measurement.

AUTHOR CONTRIBUTION

Kanakavel Kandasamy is responsible for conceptualization, Methodology, Software and Validation. Dr. James Jebaseelan Supervised the work.

ACKNOWLEDGEMENT

Thank you to Mr. Boopalan, Dr. Imthiaz & Mr. Kumaravel of KLE Society and Hospital, Belgaum, Dr. P.Mohandas Fortis Mohali for their help and guidance in this project, and special gratitude & thanks to Mr. B. Viswanathan, PTW Dosimetry India Pvt Ltd. for providing radiation detector arrays for the study.

CONFLICT OF INTEREST

There is no mention of a conflict of interest.

FINANCIAL ASSISTANCE

Nil.

REFERENCES

1. Xiao Y, Kry SF, Popple R, Yorke E, Papanikolaou N, et al. Flattening filter-free accelerators: a report from the AAPM Therapy Emerging Technology Assessment Work Group. J appli clini medi phys. 2015; 16:12-29.
2. Georg D, Knöös T, McClean B. Current status and future perspective of flattening filter-free photon beams. Med Phys. 2011; 38:1280-1293. :
3. Sharma SD. Unflattened photon beams from the standard flattening filter free accelerators for radiotherapy: Advantages, limitations, and challenges. J Med Phys. 2011; 36:123.
4. Flattening filter-free accelerators: a report from the AAPM Therapy Emerging Technology Assessment Work Group. PMC. .
5. Sudhyadhom A, Kirby N, Faddegon B, Chuang CF. Preferred dosimeter size and associated correction factors in commissioning high dose per pulse, flattening filter-free x-ray beams. Int J Med Phys Res Pract. Medical physics. 2016; 43:1507-1513.
6. Pichandi A, Kadirampatti MG, Jerina A, Balaji K, Kilaraa G. Analysis of physical parameters and determination of inflection point for Flattening Filter Free beams in medical linear accelerator. Rep Pract Oncol Radiother. 2014; 19:322-31.
7. Shende R, Gupta G, Macherla S. Determination of an inflection point for a dosimetric analysis of unflattened beam using the first principle of derivatives by python code programming. Rep Pract Oncol Radiother. 2019;24:432-442.
8. Choi MG, Law M, Yoon DK, Tamura M, Matsumoto K, et al. Simplified sigmoidal curve fitting for a 6 MV FFF photon beam of the Halcyon to determine the field size for beam commissioning and quality assurance. Radiat Oncol. 2020;15:273.
9. Muralidhar KR. Derivation of equations to define inflection point and its analysis in flattening filter free photon beams based on the principle of polynomial function. Int J Cancer Ther Oncol. 2015;3:1-5.
10. Fogliata A, Garcia R, Knöös T, Nicolini G, Clivio A, et al. Definition of parameters for quality assurance of flattening filter free (FFF) photon beams in radiation therapy. Med Phys. 2012;39:6455-64.
11. Sahani G, Sharma SD, Dash Sharma PK, Deshpande DD, Negi PS, et al. Acceptance criteria for flattening filter-free photon beam from standard medical electron linear accelerator: AERB task group recommendations. J Med Phys. 2014;39:206-11.
12. Hassn S, Deiab NA, Aly AH. Dosimetric study of photon beam characteristics with 2D array and water phantom measurement. Int J Radiat Res. 2020;18:167-72.
13. Ibrahim AG, Mohamed IE, Zidan HM. Dosimetric Comparison of Amorphous Silicon EPID and 2D Array Detector for Pre-Treatment Verification of Intensity Modulated Radiation Therapy. Int J Med Phys Clin Eng Radiat Oncol. 2018;7:438-52.
14. Decabooter E, Swinnen ACC, Öllers MC, Göpfert F, Verhaegen F. Operation and calibration of the novel PTW 1600SRS detector for the verification of single isocenter stereotactic radiosurgery treatments of multiple small brain metastases. Br J Radiol. 2021;94:20210473. Available from:
15. Ibrahim S, Seshadri V, Charles P. Assessing the suitability of a two-dimensional array for routine quality assurance checks of flatness and symmetry. Phys Eng Sci Med.2020:43:1451-1460.
16. Mhatre S. Dosimetric Comparison of a-Si 1200 and a-Si 1000 Electronic Portal Imager for Intensity Modulated Radiation Therapy (IMRT). J Nucl Med Radiat Ther. 2018;9:1-10.
17. TrueBeam_ProductBrief_RAD10128A_April2010.pdf
18. PTW Online brochure: Octavius system OCTAVIUS II | PTW
19. PTW Online brochure for Octavius 1600 SRS array; OCTAVIUS Detector 1600 SRS | PTW
20. PTW Online brochure for Starcheck array; STARCHECK | PTW
21. PTW Online brochure for Pinpoint 3D; PinPoint 3D Ion Chamber | PTW
22. PTW online brochure for RW3 slab; RW3 Slab Phantom | PTW
23. VeriSoft | PTW
24. BEAMSCAN Software | PTW
25. IAEA. Absorbed Dose Determination in External Beam Radiotherapy: An International Code of Practice for Dosimetry based on Standards of Absorbed Dose to Water IAEA TRS 398.
26. IEC. Medical electrical equipment - Medical electron accelerators - Functional performance characteristics IEC 60976:2007
27. Gandhi A, Vellaiyan S, Subramanian VS, Shanmugam T, Murugesan K, et al. Commissioning of portal dosimetry using a novel method for flattening filter-free photon beam in a nontrue beam linear accelerator. J Can Res Ther. 2019; 15:223-230.
28. PTW Manual – Beamscan Software “Analysis Parameters for FFF Photon Profiles” described in D948.131.00/09 and page No. 553
29. Pönisch F, Titt U, Vassiliev ON, Kry SF, Mohan R. Properties of unflattened photon beams shaped by a multileaf collimator. Med Phys. 2006;33:1738-46.
30. Klein EE, Hanley J, Bayouth J, Yin FF, Simon W, et al. Task Group 142 report: Quality assurance of medical accelerators a. Medi phys. 2009;36:4197-212.